J|A|C|S ARTICLES

Published on Web 05/12/2009

Versatile Coordination of 2-Pyridinetetramethyldisilazane at Ruthenium: Ru(II) vs Ru(IV) As Evidenced by NMR, X-ray, Neutron, and DFT Studies

Mary Grellier,*,† Tahra Ayed,‡ Jean-Claude Barthelat,‡ Alberto Albinati,§ Sax Mason,⊥ Laure Vendier,† Yannick Coppel,† and Sylviane Sabo-Etienne*,†

CNRS, LCC (Laboratoire de Chimie de Coordination), 205 route de Narbonne, F-31077 Toulouse, France, Université de Toulouse, UPS, INPT, F-31077 Toulouse, France, Laboratoire de Physique Quantique, IRSAMC (UMR 5626), Université Paul Sabatier, 118 route de Narbonne, 31062 Toulouse Cedex 4, France, Department of Structural Chemistry (DCSSI), University of Milan, 21, Via G. Venezian, 20133 Milan, Italy, and Institut Laue-Langevin, 6 rue Jules Horowitz, BP 156, 38042 Grenoble Cedex 9, France

Received February 13, 2009; E-mail: grellier@lcc-toulouse.fr; sylviane.sabo@lcc-toulouse.fr

Ⓦ **This paper contains enhanced objects available on the Internet at http://pubs.acs.org/jacs.**

Abstract: The novel disilazane compound 2-pyridinetetramethyldisilazane (**1**) has been synthesized. The competition between *N*-pyridine coordination and Si−H bond activation was studied through its reactivity with two ruthenium complexes. The reaction between **1** and $RuH_2(H_2)_2(PCy_3)_2$ led to the isolation of the new complex $RuH_2\{(\eta^2\text{-}HSiMe_2)N(\kappa N\text{-}C_5H_4N)(SiMe_2H)\}(PCy_3)_2$ (**2**) resulting from the loss of two dihydrogen ligands and coordination of **1** to the ruthenium center via a $\kappa^2N,(\eta^2\text{-}Si-H)$ mode. Complex **2** has been characterized by multinuclear NMR experiments (^1H, ^{31}P, ^{13}C, ^{29}Si), X-ray diffraction and DFT studies. In particular, the HMBC $^{29}Si-^1H$ spectrum supports the presence of two different silicon environments: one Si−H bond is dangling, whereas the other one is η^2-coordinated to the ruthenium with a J_{SiH} value of 50 Hz. DFT calculations (B3PW91) were also carried out to evaluate the stability of the agostic species versus a formulation corresponding to a bis(σ-Si−H) isomer and confirmed that N-coordination overcomes any stabilization that could be gained by the establishment of SISHA interactions. There is no exchange between the two Si−H bonds present in **2**, as demonstrated by deuterium-labeling experiments. Heating **2** at 70 °C under vacuum for 24 h, leads to the formal loss of one equivalent of H_2 from **2** and formation of the 16-electron complex $RuH\{(SiMe_2)N(\kappa N\text{-}C_5H_4N)(SiMe_2H)\}(PCy_3)_2$ (**3**) formulated as a hydrido(silyl) species on the basis of multinuclear NMR experiments. The dehydrogenation reaction is fully reversible under dihydrogen atmosphere. Reaction of Ru(COD)(COT) with 3 equiv of **1** under a H_2 pressure led to the isolation of the new complex $RuH\{(SiMe_2)N(\kappa N\text{-}C_5H_4N)(SiMe_2H)\}_3$ (**4**) characterized as a hydridotrisilyl complex by multinuclear NMR techniques, X-ray and neutron diffractions, as well as DFT calculations. The ^{29}Si HMBC experiments confirm the presence of two different silicon atoms in **4**, with a signal at −14.64 ppm for three dangling *Si*-Me_2H fragments and a signal at 64.94 ppm (correlating with the hydride signal) assigned to three *Si*-Me_2N groups bound to Ru. Comparison of DFT and neutron parameters involving the hydride clearly indicates an excellent correlation. The Si−H distance of ∼2.15 Å is much shorter than the sum of the van der Waals radii and typically in the range of a significant interaction between a silicon and a hydrogen atom (SISHA interactions). In **4**, three dangling Si−H groups remain accessible for further functionalization.

Introduction

Silazane $(R_3Si)_nN(R')_{3-n}$ ($n = 1-3$) compounds display a wide area of applications, from materials to organic chemistry. The 1,1,3,3-tetramethyldisilazane $(Me_2HSi)_2NR'$ family has received particular attention in recent years, due to additional reactivity that can be gained from the presence of the Si−H bonds. For example, it has been shown that they are good precursors for refractory materials,[1] surface functionalization,[2,3] silylated macromolecules,[4] or silylated organic heterocycles.[5,6]

† CNRS, LCC (Laboratoire de Chimie de Coordination), Université de Toulouse.
‡ Laboratoire de Physique Quantique, IRSAMC (UMR 5626), Université Paul Sabatier.
§ Department of Structural Chemistry (DCSSI), University of Milan.
⊥ Institut Laue-Langevin.

(1) Wrobel, A. M.; Blaszczyk, I.; Walkiewicz-Pietrzykowska, A.; Tracz, A.; Klemberg-Sapieha, J. E.; Aoki, T.; Hatanaka, Y. *J. Mater. Chem.* **2003**, *13*, 731–737.
(2) Zapilko, C.; Widenmeyer, M.; Nagl, I.; Estler, F.; Anwander, R.; Raudaschl-Sieber, G.; Groeger, O.; Engelhardt, G. *J. Am. Chem. Soc.* **2006**, *128*, 16266–16276.
(3) Giraud, L.; Jenny, T. *Organometallics* **1998**, *17*, 4267–4274.
(4) Rasul, T.; Son, D. Y. *J. Organomet. Chem.* **2002**, *655*, 115–119.
(5) Trost, B. M.; Ball, Z. T. *J. Am. Chem. Soc.* **2003**, *125*, 30–31.
(6) Tamao, K.; Nakagawa, Y.; Arai, H.; Higuchi, N.; Ito, Y. *J. Am. Chem. Soc.* **1988**, *110*, 3712–3714.

10.1021/ja901140v CCC: $40.75

Scheme 1

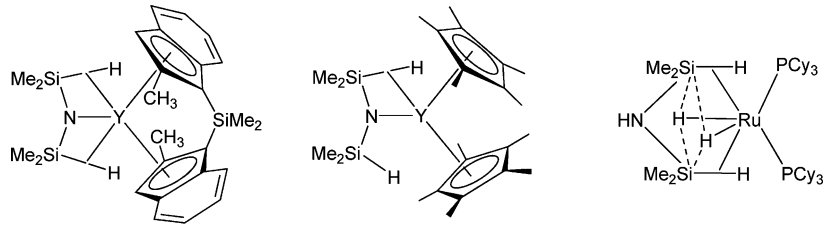

a b c

The multicenter reactivity of such ligands is well illustrated in amido lanthanidocene systems. The amidodisilazane fragment coordinates to the metal center with two or one agostic β-Si−H interactions (see Scheme 1, species **a** and **b**).[7−10] Recently, we have reported an unprecedented coordination mode of 1,1,3,3-tetramethyldisilane to ruthenium: a disilazane complex with two σ-Si−H bonds and without nitrogen coordination was isolated (Scheme 1, species **c**).[11] The stability of this coordination mode **c** could be explained by the presence of secondary interactions (SISHA) between the hydrides and the silicon atoms.[12,13] These secondary interactions are present in a wide series of silane, disilane, and disiloxane ruthenium complexes.[14] The specific coordination mode on ruthenium allowed us to achieve, in very mild conditions, catalytic selective deuteration of $NH(SiHMe_2)_2$ into $NH(SiDMe_2)_2$ under D_2 atmosphere.[11]

A good understanding of silazane coordination to a metal center is crucial to control some key steps involved in catalytic hydrosilylation processes.[15,16] There are several parameters that can be used to monitor the degree of activation of a Si−H bond between the initial step and the final one resulting in oxidative addition. In such a process and of course in the microscopic reverse reductive elimination, σ-silane complexes are often considered as intermediates.[13,17,18] Alternatively, substrate functionalization can be achieved without any change in the metal oxidation state by successive formation of σ-isomeric complexes, as recently illustrated by the concept of the σ-CAM mechanism (σ-complex assisted metathesis mechanism at late transition metals).[19] NMR is a useful technique to discriminate a σ-formulation from the corresponding product of oxidative addition. In the specific case of silane activation, ^{1}H and ^{29}Si NMR data (chemical shifts and coupling constants) can give some key information, but overlaps exist for the different classes of compounds, and the silicon substituents play also a major role. It is thus important to support the assignments by structural studies. The M−Si and Si−H bond distances are good indicators to define the activation degree of the Si−H bond. Typically, the upper limit for a σ-Si−H (or agostic) bond distance is set up at ∼1.90 Å, whereas SISHA interactions take place in the range of 2.00−2.40 Å. In the absence of neutron data, hydrogen location by X-ray diffraction is always subject to debate. In hydride and σ-complex chemistry it is thus particularly useful to perform DFT calculations as a complementary tool to support hydrogen location.[20]

Scheme 2

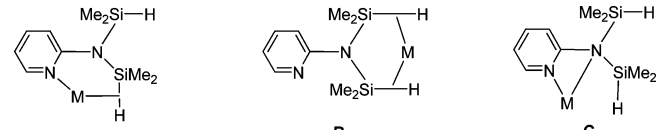

A B C

In this paper, we report the synthesis of 2-pyridinetetramethyldisilazane (**1**), a compound bearing different functionalities, and its coordination to the two ruthenium complexes, $RuH_2(H_2)_2(PCy_3)_2$ and its precursor Ru(COD)(COT). **1** is a good model to evaluate several possible chelating modes as illustrated in Scheme 2: κN,(η^2-Si−H) (**A**), bis(σ-Si−H) (**B**), and $\kappa N,N'$ (**C**). A combination of multinuclear NMR, structural and DFT studies, including a neutron determination in the case of a ruthenium (IV) hydridotrisilyl complex, allows us to discuss the activation mode of the Si−H bonds and in particular to highlight the differences between agostic η^2-Si−H bonds, SISHA interactions, and products of oxidative addition.

Results and Discussion

The synthesis of the silylated aminopyridine **1** was performed by using a standard method.[21] 2-Aminopyridine was deprotonated by one equivalent of *n*-butyllithium followed by addition of one equivalent of chlorodimethylsilane. The procedure was conducted twice to introduce a second $SiMe_2H$ fragment, but without isolating the monosilylated compound. After workup, **1** was obtained as an oily product in 86% yield. Typical NMR patterns for $RNSiMe_2H$ fragments were obtained for **1**: a high-field ^{29}Si resonance at −11.21 ppm and in the ^{1}H NMR spectrum a septet at 4.97 ppm ($^3J_{HH}$ = 3.3 Hz and $^1J_{SiH}$ = 191.6 Hz) for the Si−H groups and four pyridinic-proton signals at 8.10, 7.06, 6.71, and 6.39 ppm.

(7) Klimpel, M. G.; Gorlitzer, H. W.; Tafipolsky, M.; Spiegler, M.; Scherer, W.; Anwander, R. *J. Organomet. Chem.* **2002**, *647*, 236–244.
(8) Eppinger, J.; Spiegler, M.; Hieringer, W.; Herrmann, W. A.; Anwander, R. *J. Am. Chem. Soc.* **2000**, *122*, 3080–3096.
(9) Herrmann, W. A.; Eppinger, J.; Spiegler, M.; Runte, O.; Anwander, R. *Organometallics* **1997**, *16*, 1813–1815.
(10) Otero, A.; Fernandez-Baeza, J.; Lara-Sanchez, A.; Alonso-Moreno, C.; Marquez-Segovia, I.; Sanchez-Barba, L. F.; Rodriguez, A. M. *Angew. Chem., Int. Ed.* **2009**, *121*, 2210−2213.
(11) Ayed, T.; Barthelat, J.-C.; Tangour, B.; Pradère, C.; Donnadieu, B.; Grellier, M.; Sabo-Etienne, S. *Organometallics* **2005**, *24*, 3824–3826.
(12) Atheaux, I.; Delpech, F.; Donnadieu, B.; Sabo-Etienne, S.; Chaudret, B.; Hussein, K.; Barthelat, J. C.; Braun, T.; Duckett, S. B.; Perutz, R. N. *Organometallics* **2002**, *21*, 5347–5357.
(13) Lachaize, S.; Sabo-Etienne, S. *Eur. J. Inorg. Chem.* **2006**, 2115–2127.
(14) Delpech, F.; Sabo-Etienne, S.; Daran, J. C.; Chaudret, B.; Hussein, K.; Marsden, C. J.; Barthelat, J. C. *J. Am. Chem. Soc.* **1999**, *121*, 6668–6682.
(15) Marciniec, B. *Coord. Chem. Rev.* **2005**, *249*, 2374–2390.
(16) Marciniec, B. In *Applied Homogeneous Catalysis with Organometallic Compounds*, 2nd ed.; Cornils, B., Herrmann, W. A., Eds.; Wiley-VCH: Weinheim, 2002; p 491.
(17) Corey, J. Y.; Braddock-Wilking, J. *Chem. Rev.* **1999**, *99*, 175–292.
(18) Kubas, G. J. *Metal Dihydrogen and σ-Bond Complexes*; Kluwer Academic/Plenum Publishers: New York, 2001.
(19) Perutz, R. N.; Sabo-Etienne, S. *Angew. Chem., Int. Ed.* **2007**, *46*, 2578–2592.
(20) Alcaraz, G.; Sabo-Etienne, S. *Coord. Chem. Rev.* **2008**, *252*, 2395–2409.
(21) Wiseman, G. H.; Wheeler, D. R.; Seyferth, D. *Organometallics* **1986**, *5*, 146–152.

Scheme 3

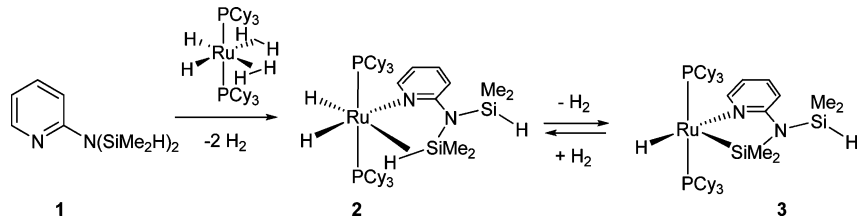

Reaction of 2-Pyridinetetramethyldisilazane (1) with $RuH_2(H_2)_2(PCy_3)_2$. We have previously demonstrated that the bis(dihydrogen) complex $RuH_2(H_2)_2(PCy_3)_2$ is the precursor of choice to prepare a series of bis(silane) complexes of general formula $RuH_2\{(\eta^2\text{-}HSiMe_2)Z\}_2(PCy_3)_2$. When the spacer linking the two silicons is larger than one atom ($Z = C_6H_4$, $(CH_2)_n$, $OSiMe_2O$) a similar structure was observed with two (η^2-Si−H) in a trans configuration,[14,22] whereas in the case of a short spacer (Z = O, NH) the two (η^2-Si−H) are in a cis configuration due to a steric constraint.[11,12] The reaction between **1** and $RuH_2(H_2)_2(PCy_3)_2$ leads to the isolation of a new complex $RuH_2\{(\eta^2\text{-}HSiMe_2)N(\kappa N\text{-}C_5H_4N)(SiMe_2H)\}(PCy_3)_2$ (**2**) resulting from the loss of two dihydrogen ligands and coordination of **1** to the ruthenium center via a κ^2N,(η^2-Si−H) **A** mode (see Schemes 2 and 3). Complex **2** has been characterized by multinuclear NMR experiments and X-ray diffraction. At room temperature, the ^{1}H NMR spectrum in C_6D_6 exhibits four signals at 9.31, 6.60, 6.48, 5.90 ppm, characteristic of a pyridine group coordinated to a ruthenium center (the ortho proton of the pyridine fragment is deshielded by 1.20 ppm compared to the free ligand **1**). The HMBC ^{29}Si−^{1}H spectrum supports the presence of two different silicon environments. The dangling Si−H^b group is characterized by a ^{29}Si NMR high field signal at −14.5 ppm and by a septet in the ^{1}H NMR spectrum integrating for one hydrogen at 5.33 ppm ($^1J_{HSi}$ = 207 Hz) as well as a doublet integrating for six hydrogen atoms at 0.40 ppm. The singlet integrating for six hydrogens at 1.10 ppm correlates with a silicon resonance at 56.9 ppm and is characteristic of a Si coordinated to a ruthenium center. At 298 K, the upfield region in the ^{1}H NMR spectrum is almost featureless as a result of a fast exchange between the different hydrogen atoms coordinated to ruthenium (Figure 1). At 223 K, three upfield signals of equal intensity at −3.79, −10.70, −13.55 ppm are well-resolved and assigned to H^c, H^a and H^d, respectively, on the basis of the following experiments: (i) by recording a ^{1}H{^{31}P} NMR spectrum the triplet at −3.79 turns into a singlet, the multiplet at −10.70 leads to a doublet with a $^2J_{HH}$ = 10 Hz and the doublet of triplet at −13.55 simplifies into a doublet with also a $^2J_{HH}$ = 10 Hz. (ii) 1D NOE ^{1}H NMR experiments with a mixing time of 300 ms show that only the hydride at −3.79 ppm is close to the ortho pyridinic hydrogen. (iii) The HMBC ^{29}Si−^{1}H experiment reveals a correlation between the silicon at 56.9 ppm and the hydride at −10.70 ppm, whereas a homodecoupled ^{1}H{^{31}P} NMR on the signal at −13.55 ppm turns the signal at −10.70 ppm into a singlet and allows the measurement of the silicon satellites. The J_{SiH} value of 50 Hz is in the range characteristic of σ-silane complexes and thus indicates a significant activation of the Si−H bond.[23] Finally, at higher temperatures, exchange of the three hydrides is observed with an estimated $\Delta G^{\ddagger}$ of 51 kJ·mol^{-1} at 313 K leading at 333 K to a very broad signal at −10 ppm. On the basis of these ^{1}H, ^{29}Si and ^{31}P NMR studies at various temperatures, we can propose a structure consistent with the ruthenium surrounded by two equivalent phosphine ligands, a N pyridinic atom, two hydrides and one η^2-Si−H on the ruthenium as described in Scheme 3. Such a formulation is confirmed by an X-ray diffraction analysis (see Table 1). The X-ray structure is depicted in Figure 2, and the most relevant geometrical parameters are reported in Table 2.

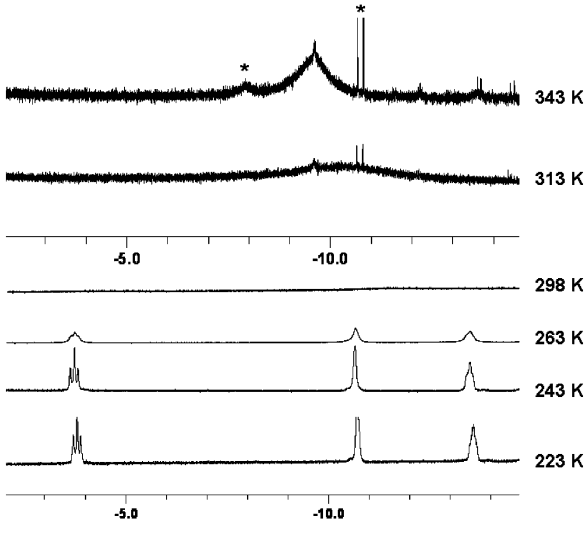

Figure 1. Variable-temperature ^{1}H NMR (400 MHz) spectra of **2** in C_7D_8 in the hydride region (* indicates impurities).

The crystal structure of **2** is characterized by a symmetry plane through the pyridinic ring, the disilazane fragment and the ruthenium-hydrides core. The two tricyclohexylphosphines are in a trans configuration with a P−Ru−P angle bent toward the hydrides (155.71 (3)°). The three hydrides could be located, and DFT calculations support their location (see below). The Si1−H1^a bond is η^2-coordinated to the ruthenium center as illustrated by the bond distances of Ru−Si1 2.415(1) Å, Ru−H1^a 1.66 (4) Å and Si1−H1^a 1.63(4) Å. The Si1−H1^a bond distance is longer than that in the dangling Me_2SiH group (Si2−H1^b of 1.44(5) Å). The η^2-Si−H distance is in the lower limit of the range reported for a series of σ-Si−H ruthenium complexes,[17,18,24] and close to the values found in a bis(cyclometalated) ruthenium complex displaying two β-agostic Si−H bonds (1.76(4) Å and 1.65(3) Å).[25] Because of the problems associated with the hydride location by X-ray diffraction, we carried out a DFT optimization of **2** without any simplification and using B3PW91 as a functional. A good correlation was found between the X-ray data for **2** and the calculated geometrical parameters for **2a** as can be seen from Table 2. The Ru−Si distance in particular is

(22) Delpech, F.; Sabo-Etienne, S.; Chaudret, B.; Daran, J.-C. *J. Am. Chem. Soc.* **1997**, *119*, 3167–3168.
(23) Alcaraz, G.; Helmstedt, U.; Clot, E.; Vendier, L.; Sabo-Etienne, S. *J. Am. Chem. Soc.* **2008**, *130*, 12878–12879.
(24) Schubert, U. *Adv. Organomet. Chem.* **1990**, *30*, 151–187.
(25) Montiel-Palma, V.; Munoz-Hernandez, M. A.; Ayed, T.; Barthelat, J.-C.; Grellier, M.; Vendier, L.; Sabo-Etienne, S. *Chem. Commun.* **2007**, 3963–3965.

Table 1. Crystal Data and Details of the Structure Refinement for **2** and **4** (X-ray and Neutron Diffraction)

	2 (X-ray)	**4** (X-ray)	**4** (neutron)
formula	$C_{45}H_{86}N_2P_2RuSi_2$	$C_{27}H_{52}N_6RuSi_6$	$C_{27}H_{52}N_6RuSi_6$
molecular weight	874.35	730.33	730.33
temperature, K	160(2)	110(2)	20(1)
diffractometer	XCALIBUR	XCALIBUR	ILL D19
radiation	Mo Kα (λ = 0.71073 Å)	Mo Kα (λ = 0.71073 Å)	neutron (λ = 1.1695(1) Å)
crystal system	monoclinic	trigonal	trigonal
space group (no.)	$P2_1/m$ (10)	$R\bar{3}$ (148)	$R\bar{3}$ (148)
a, Å	9.831(2)	18.645(2)	18.5880(3)
b, Å	21.651(4)	18.645(2)	18.5880(3)
c, Å	11.917(2)	19.061(2)	18.8361(3)
α, deg	90	90	90
β, deg	109.44(3)	90	90
γ, deg	90	120	120
V, Å^3	2391.9(9)	5739(1)	5636.2(2)
Z	2	6	6
ρ_{calcd}, g cm^{-3}	1.214	1.268	1.290
μ, mm^{-1}	0.476	0.623	0.201
θ range (deg)	3.41−26.37	3.31−25.68	2.74−61.69
no. reflns collected	34507	7095	13183
no. independ. reflns	4805	2409	4285
observed reflns	4391	1598	3216
R_{int}[a]	0.046	0.051	0.097
$R(F_o)$ [$I > 2\sigma(I)$]	0.0403	0.0361	0.0698
R_w (F_o^2) [$I > 2\sigma(I)$][b]	0.0912	0.0566	0.1306
GOF	1.101	0.894	1.119

[a] $R_{int} = \Sigma|F_o^2 - \langle F_o\rangle|/\Sigma F_o^2$; $R(F_o) = \Sigma||F_o| - |F_c||/\Sigma|F_o|$. [b] $R_w(F_o^2) = [\Sigma[w(F_o^2 - F_c^2)^2]/\Sigma[w(F_o^2)^2]]^{1/2}$; GOF = $[\Sigma[w(F_o^2 - F_c^2)^2]/(N - P)]^{1/2}$, where N, P are the number of observations and parameters, respectively.

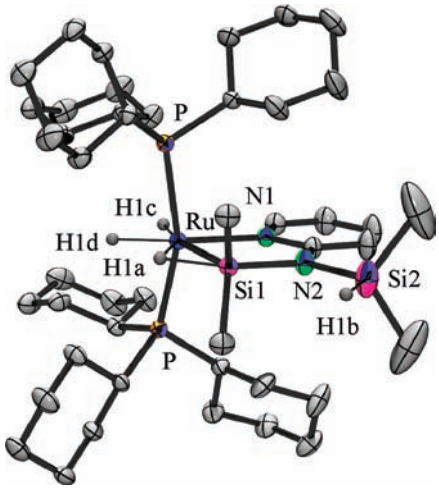

Figure 2. X-ray structure of compound **2**. Thermal ellipsoids are shown at the 50% probability level. All the hydrogen atoms are omitted for clarity except those bound to the ruthenium.

well reproduced as well as the P−Ru−P angle. The η^2-Si−H coordination is confirmed by DFT with a significant lengthening of the Si−H bond: 1.840 Å. This value, longer than the measured X-ray distance, indicates a substantial activation of the Si−H bond in agreement with the J_{SiH} value of 50 Hz. Moreover, theoretical calculations were carried out to evaluate the stability of the agostic species **2a** versus a formulation corresponding to a bis(σ-Si−H) isomer. As mentioned in the introduction, we have already demonstrated that such a structure with two σ-Si−H bonds in a cis position ($RuH_2\{(\eta^2\text{-}HSiMe_2)_2NH\}(PCy_3)_2$) could be obtained.[11] Here, we did not use any simplified model, and the calculations were carried out at the B3PW91 level. As depicted in Figure 3, two other isomers were optimized to a local minimum: complex **2a** (**A** coordination mode, Scheme 2) corresponding to the X-ray structure is the lowest in energy, whereas complexes **2b** and **2c** are 48 kJ·mol^{-1} and 51 kJ·mol^{-1} less stable than **2a**, respectively. Isomer **2b** displays a **B** coordination mode (Scheme 2) with a geometry very similar to the X-ray structure reported for the disilazane complex $RuH_2\{(\eta^2\text{-}HSiMe_2)_2NH\}(PCy_3)_2$. The two phosphines are in a cis position to allow the formation of two σ-Si−H bonds (Si1−H1[a] = 1.963 and Si2−H1[b] = 1.819 Å) and four SISHA interactions (Si···H distances ∼2.3 Å). In **2c**, the phosphines are in a trans position, thus preventing any stabilization by SISHA interactions (Si···H distances > 3.4 Å), and the activation degree of the two Si−H bonds is quite different as demonstrated by the different values obtained for the Ru−Si and Si−H distances (Table 2).

Table 2. Comparison between Selected Geometrical Parameters (distances in Å, angles in deg) for the Experimental X-ray **2** and Calculated **2a**−**c** (DFT/B3PW91) Structures

	2 (X-ray)	**2a** (DFT)	**2b** (DFT)	**2c** (DFT)
Ru−H1[a]	1.66(4)	1.632	1.608	1.655
Ru−H1[b]			1.700	1.715
Ru−H1[c]	1.62(4)	1.634	1.648	1.602
Ru−H1[d]	1.54(4)	1.603	1.605	1.620
Ru−Si1	2.4150(14)	2.418	2.422	2.492
Ru−Si2			2.434	2.878
Si1−H1[a]	1.63(4)	1.840	1.963	1.751
Si2−H1[b]	1.44(5)	1.488	1.819	1.600
Si1−H1[c]			2.403	3.527
Si1−H1[d]			2.156	4.059
Si2−H1[a]			2.405	3.776
Si2−H1[d]			2.301	3.443
Ru−N1	2.191(3)	2.215		
P−Ru−P	155.71(3)	155.36	114.55	150.23
H1[a]−Ru−Si1	42.2(13)	49.52	53.81	44.50
H1[b]−Ru−Si2			48.32	28.61
N−Ru−Si	78.79(9)	79.00		

It is noteworthy that nitrogen coordination of a N sp^2 involved in an aromatic ring such as pyridine or quinoline is highly favored.[26,27] In the present system, N-coordination overcomes any stabilization that could be gained by the establishment of SISHA interactions. Our calculations allow us to estimate the energy difference between an agostic Si−H bond and a bis σ-Si−H formulation. They are also useful to support IR assignment for the Ru−H and Ru−H−Si stretching modes.[14] Indeed, the IR spectrum (Nujol) of **2** displays three medium bands in the range 2200−1890 cm^{-1}. The two bands at 2191 cm^{-1} and 1987 cm^{-1} are assigned to the H−Si stretch of the dangling $SiMe_2H$ group and the Ru−H stretches, respectively, whereas the broadband at 1897 cm^{-1} corresponds to a mixing of Ru−H and Ru−H−Si stretches.

Even though **2** is very stable in the solid state, we noticed some decomposition upon storage, over a long period, at room

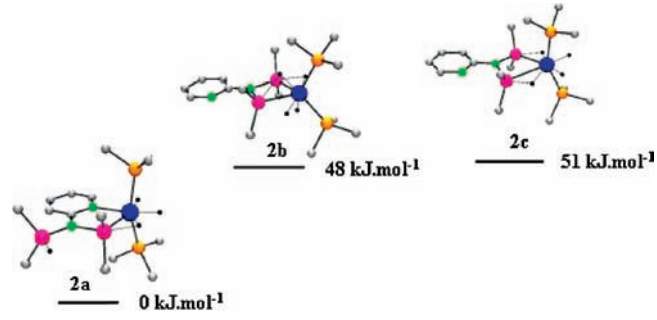

Figure 3. Three B3PW91-optimized isomeric structures of **2**. Carbons are in gray, silicons in pink, nitrogens in green, phosphorus atoms in orange, ruthenium atoms in blue and hydrogen atoms in black. For clarity, only the C attached to P of the tricyclohexylphosphines have been represented.

Scheme 4

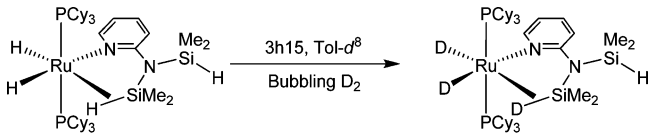

temperature under an argon atmosphere (33% decomposition in 2 years!). A new complex was detected by NMR that could be isolated as an orange solid on a preparative scale by heating **2** at 70 °C under vacuum for 24 h. The thermal decomposition is quantitative and corresponds to the formal loss of one equivalent of H_2 from **2**. The new complex $RuH\{(SiMe_2)N(\kappa N\text{-}C_5H_4N)(SiMe_2H)\}(PCy_3)_2$ (**3**) is formulated as a hydrido(silyl) species on the basis of multinuclear NMR experiments (see Scheme 3). The $^{31}P\{^1H\}$ NMR spectrum exhibits one singlet at 52.7 ppm consistent with two equivalent phosphines. In the ^1H NMR spectrum, the hydrogen in the ortho position of the pyridinic fragment is shielded at 8.74 ppm. The three other hydrogen atoms of the aromatic ring are deshielded by ~0.35 ppm compared to compound **2**. The HMQC $^{29}Si-^1H$ experiment shows two silicon resonances at −16.6 ppm for the dangling SiH and 64.1 ppm for the silyl group ($Ru-SiMe_2$). In the hydride region, only one triplet is observed at −12.70 ppm ($^2J_{HP}$ = 25 Hz). The $^1H\{^{31}P\}$ NMR experiment allows the detection of the silicon satellites and a $^2J_{SiH}$ value of 11 Hz can be measured. All the data are in agreement with the formation of a hydrido(silyl) complex. The silyl group which is the strongest σ-donor ligand is trans to the vacant site.[28]

The dehydrogenation process is fully reversible. Thus, bubbling H_2 in a C_6D_6 solution of **3** allows total conversion to **2**, as monitored by ^1H and ^{31}P NMR. We then examined the behavior of a C_7D_8 solution of **2** under D_2 atmosphere. After bubbling D_2 for 3.25 h, NMR monitoring showed 53% of deuterium incorporation into the two hydrides and the η^2-Si−H bond (see Scheme 4). No deuterium incorporation was detected in the dangling Si−H bond. This observation confirms that there is no exchange between the two Si−H bonds present in **2**. This opens some possibilities for further functionalization of the dangling Si−H group, for example by hydrosilylation.

Reaction of 2-Pyridinetetramethyldisilazane (1) with Ru(COD)(COT). In view of the reversible dehydrogenation process between **3** and **2**, it was tempting to test the reactivity of **1** with Ru(COD)(COT), the precursor for the synthesis of the bis(dihydrogen) complex $RuH_2(H_2)_2(PCy_3)_2$. In that context, oxidative addition of the Si−H bonds could compete toward N-coordination. Reaction of Ru(COD)(COT) with 3 equiv of **1** under a H_2 pressure for a few minutes, led after workup to the isolation of the new complex $RuH\{(SiMe_2)N(\kappa N\text{-}C_5H_4N)(SiMe_2H)\}_3$ (**4**) (Scheme 5) characterized as a hydridotrisilyl ruthenium (IV) complex by multinuclear NMR techniques, X-ray and neutron diffractions, as well as DFT calculations.

In the hydride region, the ^1H NMR spectrum of **4** shows one singlet at −13.63 ppm displaying silicon satellites with an

Scheme 5

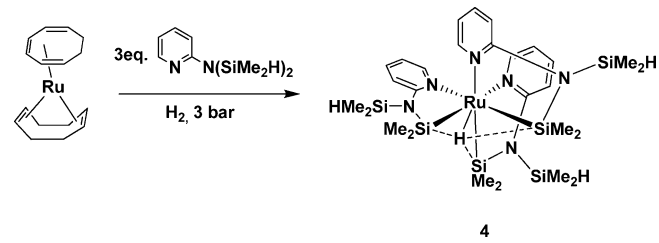

Table 3. Comparison between Selected Geometrical Parameters for Compound **4** Obtained from X-ray and Neutron Diffraction As Well As DFT Calculations (distances in Å, angles in deg).

4	X-ray	neutron	DFT
Ru−H10	1.41(5)	1.559(7)	1.557
Ru−Si1	2.3291(9)	2.326(3)	2.346
Si1−H10	2.120(9)	2.154(8)	2.162
Si2−H11	1.45(3)	1.481(5)	1.491
Ru−N1	2.231(2)	2.226(2)	2.246
N1−Ru−Si1	80.32(6)	80.12(6)	79.98
H10−Ru−Si1	63.59(3)	63.81(8)	63.56
H10−Ru−N1	124.76(6)	124.86(6)	124.98

apparent coupling constant J_{HSiapp} of 7.5 Hz. All the integration ratios are in agreement with the presence of three pyridinic, three $SiMe_2H$ and three $SiMe_2$ fragments for only one hydride. Methyl substituents on the silicon atoms are diastereotopic. The ^{29}Si HMBC experiments confirm the presence of two different silicon atoms in **4**. The signal at −14.24 ppm is assigned to three dangling $SiMe_2H$ fragments, whereas the signal at 64.94 ppm which correlates with the hydride signal is assigned to three $SiMe_2N$ groups bound to Ru.

After having obtained crystals for X-ray diffraction, it was also possible to grow a few crystals suitable for neutron diffraction. Selected distances and angles are listed in Table 3, as well as those calculated from the corresponding theoretical model. An ORTEP view of the neutron structure is shown in Figure 4.

As already mentioned above, hydrogen location by X-ray diffraction is difficult and subject to systematic errors always

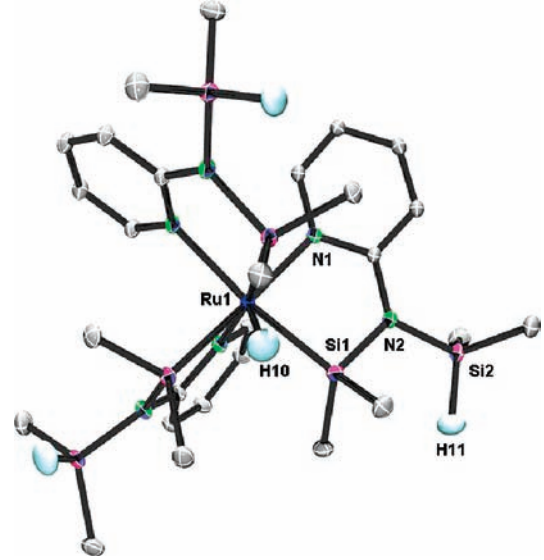

Figure 4. Neutron structure of $RuH\{(SiMe_2)N(\kappa N\text{-}C_5H_4N)(SiMe_2H)\}_3$ (**4**). Movie in GIF format of neutron structure of **4**. All the hydrogen atoms are omitted for clarity, except those on ruthenium and silicon atoms.

(26) Matthes, J.; Gründemann, S.; Toner, A.; Guari, Y.; Donnadieu, B.; Spandl, J.; Sabo-Etienne, S.; Clot, E.; Limbach, H. H.; Chaudret, B. *Organometallics* **2004**, *23*, 1424–1433.
(27) Toner, A.; Matthes, J.; Grundemann, S.; Limbach, H. H.; Chaudret, B.; Clot, E.; Sabo-Etienne, S. *Proc. Natl. Acad. Sci. U.S.A.* **2007**, *104*, 6945–6950.
(28) Lachaize, S.; Caballero, A.; Vendier, L.; Sabo-Etienne, S. *Organometallics* **2007**, *26*, 3713–3721.

leading to an underestimation of the M−H distances. However, we and others have found that useful and reliable information can, nonetheless, be obtained from this technique by combining the X-ray results with those from DFT calculations.[13,20,29] Here, we had a unique opportunity to compare X-ray, neutron and DFT values. We have thus performed a DFT/B3PW91 calculation on **4** without any simplification on the model used. Table 3 allows a direct comparison of some selected values obtained by the three methods. The Ru−H distance of 1.41(5) Å by X-ray, and 1.559(7) Å by neutron, can be compared to the median value of 1.59 Å for terminal Ru−H distances obtained by X-ray diffraction from the Cambridge Structural Data Center. Four neutron diffraction structures of ruthenium complexes with a terminal hydride have been previously reported: the cationic complex $[RuH(H_2)(dppe)_2][BF_4]$ displays a Ru−H distance of 1.64(2) Å,[30] whereas slightly shorter values have been found in $CpRuH(PMe_3)_2$ (1.630(4) Å), $[CpRuH_2(PMe_3)_2][BF_4]$ (1.599(8) Å and 1.604(9) Å, respectively),[31] and $RuH_2(H_2)_2(PCyp_3)_2$ (1.628(4) Å 1.625(4) Å).[32] As expected, X-ray Ru−H distances are systematically shorter than those from neutron. The Ru−Si distance is 2.3291(9) Å by X-ray and 2.326(3) Å by neutron. This is a rather short distance, but in the range found for 58 Si attached to ruthenium complexes from the CSD (in the range 2.19−2.47 Å) with a median value of 2.43 Å. Comparison of DFT and neutron parameters involving the hydride clearly indicates an excellent correlation. The Si−H distance of ∼2.15 Å is much shorter than the sum of the van der Waals radii and typically in the range of a significant interaction between a silicon and a hydrogen atom (SISHA).[12,13] It is worth noting that all the Ru−H bonds reported in the CSD refer to octahedral complexes with a defined trans ligand to the hydride. In our case, the Ru−H vector is pointing to the middle of the triangular face defined by the three symmetry-related Si atoms bonded to Ru. We are in presence of a seven-coordinated ruthenium: a capped octahedron which is unprecedented for mononuclear neutral Ru complexes.

Conclusion

We have synthesized a new silylated aminopyridine compound **1** which allows us to tune the Si−H bond activation upon coordination to a ruthenium center. Three new ruthenium complexes have been prepared in which N-coordination of the pyridine group is always favored, no matter the ruthenium oxidation state and the number of ligands around the metal. By addition to the bis(dihydrogen) complex $RuH_2(H_2)_2(PCy_3)_2$ we could form either a dihydride ruthenium (II) complex **2** stabilized by an agostic Si−H interaction or an unsaturated hydrido(silyl) 16-electron species **3**. The hydrogenation/dehydrogenation process is fully reversible under a dihydrogen atmosphere. Interestingly, deuterium incorporation in **2** is selective with isotopic labeling occurring only at hydrogen atoms bound to the metal.

Access to the first hydridotrisilyl ruthenium (IV) complex **4** was possible by direct reaction of **1** with Ru(COD)(COT). The reaction performed under dihydrogen atmosphere allows alkene ligand hydrogenation and access to the Ru center. We have obtained the first neutron structure of a ruthenium silyl complex which moreover has three silyl groups in the coordination sphere of the metal. The synthesis of such a complex with a general formulation $RuH(SiR_3)_3L_3$ is particularly interesting in view of the controversial discussions on the analogous trihydride(silyl) $RuH_3(SiR_3)L_3$ family.[13,33−40] In our system, a ruthenium (IV) formulation is highly favored, leading to the formation of three Ru−Si bonds. The short Ru−Si and Ru−H distances are in agreement with such a formulation, and the Si−H bond distances are characteristic of secondary interactions (SISHA) between the hydride and the three silicon atoms. It is noteworthy that the J_{SiH} value in **4** is comparable to typical J_{SiH} values for a coupling between methyl protons bound to silicon atoms.

The Si−H bond activation by coordination of **1** to a ruthenium center can thus range from an agostic level to a full oxidative addition process, but the formation of a "true" σ-complex is avoided, N-coordination of the pyridine fragment being predominant. Our study combining X-ray, neutron and DFT data gives again more credit to the location of hydrogen atoms by X-ray. Caution should remain, however, but geometrical parameters obtained from the combined use of low-temperature X-ray data on high-quality crystals and DFT calculations seem to be quite reliable. Finally, it is worth pointing out that in **4**, three dangling Si−H groups remain accessible for further functionalization as well as for grafting the organometallic fragment into various supports. More generally, in suitable conditions, addition of different substrates to the ruthenium (0) precursor Ru(COD)(COT) could lead to the access of new species for applications in catalysis or materials science.

Experimental Section

All reactions and workup procedures were performed under an argon atmosphere using a conventional vacuum line and Schlenk tube techniques or in a drybox. Solvents were dried and freshly distilled according to standard procedures and degassed prior to use. $RuH_2(H_2)_2(PCy_3)_2$ and Ru(COD)(COT) were prepared according to published procedures.[41,42] All NMR solvents were dried and degassed using appropriated methods. NMR spectra were acquired on Bruker AC 200, AV 300, Avance 400 and Avance 500 spectrometers. GC/MS analysis and microanalysis were performed by the Laboratoire de Chimie de Coordination Microanalytical Service. The GC/mass spectra were measured at 70 eV on a HP 5973 attached to a HP 6890 (capillary column HP-5MS, 30 m, 0.25 mm, 0,250 mm with a temperature ramp 80 °C (2 min); 10 °C/min; 280 °C (5 min)). Infrared spectra were obtained as Nujol mulls on a Perkin-Elmer 1725 FT-IR spectrometer.

(29) Maseras, F.; Lledos, A.; Clot, E.; Eisenstein, O. *Chem. Rev.* **2000**, *100*, 601–636.
(30) Albinati, A.; Klooster, W. T.; Koetzle, T. F.; Fortin, J. B.; Ricci, J. S.; Eckert, J.; Fong, T. P.; Lough, A. J.; Morris, R. H.; Golombek, A. P. *Inorg. Chim. Acta* **1997**, *259*, 351–357.
(31) Brammer, L.; Klooster, W. T.; Lemke, F. R. *Organometallics* **1996**, *15*, 1721–1727.
(32) Grellier, M.; Vendier, L.; Chaudret, B.; Albinati, A.; Rizzato, S.; Mason, S.; Sabo-Etienne, S. *J. Am. Chem. Soc.* **2005**, *127*, 17592–17593.
(33) Yardy, N. M.; Lemke, F. R.; Brammer, L. *Organometallics* **2001**, *20*, 5670–5674.
(34) Dioumaev, V. K.; Yoo, B. R.; Procopio, L. J.; Carroll, P. J.; Berry, D. H. *J. Am. Chem. Soc.* **2003**, *125*, 8936–8948.
(35) Hübler, K.; Hübler, U.; Roper, W. R.; Schwerdtfeger, P.; Wright, L. J. *Chem.−Eur. J.* **1997**, *3*, 1608–1616.
(36) Mohlen, M.; Rickard, C. E. F.; Roper, W. R.; Salter, D. M.; Wright, L. J. *J. Organomet. Chem.* **2000**, *593−594*, 458–464.
(37) Hussein, K.; Marsden, C. J.; Barthelat, J. C.; Rodriguez, V.; Conejero, S.; Sabo-Etienne, S.; Donnadieu, B.; Chaudret, B. *Chem. Commun.* **1999**, 1315–1316.
(38) Nikonov, G. I. *Angew. Chem., Int. Ed.* **2001**, *40*, 3353–3355.
(39) Dioumaev, V. K.; Procopio, L. J.; Carroll, P. J.; Berry, D. H. *J. Am. Chem. Soc.* **2003**, *125*, 8043–8058.
(40) Lachaize, S.; Sabo-Etienne, S.; Donnadieu, B.; Chaudret, B. *Chem. Commun.* **2003**, 214–215.
(41) Borowski, A. F.; Sabo-Etienne, S.; Christ, M. L.; Donnadieu, B.; Chaudret, B. *Organometallics* **1996**, *15*, 1427–1434.
(42) Pertici, P.; Vitulli, G.; Paci, M.; Porri, L. *J. Chem. Soc., Dalton Trans.* **1980**, 1961–1964.

Synthesis and Characterization of 2-Pyridinetetramethyldisilazane (1). To a solution of 2-aminopyridine (3.00 g, 31.3 mmol) in diethyl ether (100 mL) at 0 °C in a 250 mL round flask Schlenk, 20 mL of *n*-BuLi (1.6 M in hexane) was added. This solution was stirred for 2 h at 0 °C. A solution of $HSiMe_2Cl$ (3.5 mL, 31.5 mmol) in 20 mL of diethyl ether was added slowly to the previous solution at 0 °C leading the formation of a precipitate. This mixture was stirred for 2 h at 0 °C. After this period, another equivalent of *n*-BuLi (20 mL, 1.6 M in hexane) was added to the suspension and maintained at 0 °C. After 2 h of stirring at this temperature, another one equivalent of $HSiMe_2Cl$ (3.5 mL, 31.5 mmol) was added. The suspension was allowed to return to room temperature and was stirred for 48 h. The mixture was filtered, and the white solid was washed with 2 × 20 mL of Et_2O. The collected solutions were combined, and the solvent was evaporated to dryness. The resulting oil was distillated by trap-to-trap technique. The pale-yellow oil was isolated in 86% yield (5.62 g).

^{1}H NMR (200.13 MHz, C_6D_6, 298 K): 8.10 (ddd, 1 H, Pyr, $^3J_{HH}$ = 5.0, $^4J_{HH}$ = 2.0, $^5J_{HH}$ = 1.0), 7.06 (ddd, 1 H, Pyr, $^3J_{HH}$ = 8.3, $^3J_{HH}$ = 7.2, $^4J_{HH}$ = 2), 6.71 (dt, 1 H, Pyr, $^3J_{HH}$ = 8.3, $^4J_{HH}$ = 1.0, $^5J_{HH}$ = 1.0), 6.39 (ddd, 1 H, Pyr, $^3J_{HH}$ = 7.2, $^3J_{HH}$ = 5.0, $^4J_{HH}$ = 1.0), 4.97 (sept, 2 H, SiH, $^3J_{HH}$ = 3.3, $^1J_{HSi}$ = 191.6), 0.48 (d, 12 H, $SiMe_2$, $^3J_{HH}$ = 3.3). ^{13}C{^{1}H} NMR (50.32 MHz, C_6D_6, 298 K): 161.0, 147.0, 136.8, 114.5, 112.3 (all for Pyr), −0.8 (4C, $SiMe_2H$). ^{29}Si INEPTRD NMR (99.39 MHz, C_6D_6, 298 K): −11.21 (s). IR (Nujol mulls, cm^{-1}) 2135 (s, νSi−H). EI-MS: *m*/*z* 209 (M − 1).

Synthesis and Characterization of $RuH_2(\eta^2$-$HSiMe_2)(N$-{$(C_5H_4N)(SiMe_2H)$}$)(PCy_3)_2$ (2). One equivalent of **1** was added to a suspension of $RuH_2(H_2)_2(PCy_3)_2$ (62 mg, 93 μmol) in 5 mL of pentane. The solution became homogeneous, and after 5 min a precipitate appeared. The solid was separated from the solution and washed with 3 × 1.5 mL of pentane and dried under vacuum. **2** was obtained as a pale-yellow solid in 50% isolated yield.

^{1}H NMR (400.13 MHz, Tol-d_8, 223 K): 9.31 (d, 1 H, Pyr, $^3J_{HH}$ = 5.2), 6.60 (t, 1 H, Pyr, $^3J_{HH}$ = 7.2), 6.48 (d, 1 H, Pyr, $^3J_{HH}$ = 8.4), 5.90 (t, 1 H, Pyr), 0.5.33 (sept, 1 H, SiH, $^3J_{HH}$ = 3.6, $^1J_{HSi}$ = 207), 3.00−1.00 (m, 66H, PCy_3), 1.10 (s, 6H, Ru−$SiMe_2$); 0.40 (d, 6 H, HSi$\underline{Me}_2$). −3.79 (t, RuH, $^2J_{HP}$ = 27.2), −10.70 (m, 1H, RuH, $^2J_{HP}$ = 9.5, $^2J_{HH}$ = 9.5), −13.55 (dt, 1H, RuH, $^2J_{HP}$ = 21.5, $^2J_{HH}$ = 9.5). ^{13}C{^{1}H} NMR (160.62 MHz, Tol-d_8, 298 K): 166.64, 160.32, 133.71, 111.23, 110.93 (all for Pyr), 35.49 (t, $^1J_{PC}$ = 9.1, PCH), 31.57, 29.58, 28.11, 27.08 (CH_2 of PCy_3), 13.99 (t, $^3J_{CP}$ = 4.1, $SiMe_2Ru$), −2.49 ($SiMe_2H$). ^{31}P{^{1}H} NMR (161.97 MHz, Tol-d_8, 223 K): 66.6 (s, PCy_3); ^{29}Si {^{31}P 66.6 ppm} HMQC NMR (99.39 MHz, Tol-d_8, 223 K): −14.5 ($SiMe_2H$), 56.9 (Ru−$SiMe_2$). IR (Nujol mulls, cm^{-1}) 2191(m, νSi−H dangling), 1987 (m, νRu−H), 1897 (m br, νRu−H + νRu−H−Si). We are confident in the band assignments by comparison to the values obtained from DFT calculations.

Anal. Calcd for $RuC_{45}H_{86}N_2Si_2P_2$: C, 61.81; H, 9.91; N, 3.20. Found: C, 61.83; H, 9.98; N, 3.00.

Synthesis and Characterization of RuH{$(SiMe_2)N(\kappa N$-$C_5H_4N)$-$(SiMe_2H)$}$(PCy_3)_2$ (3). The complex was prepared by heating **2** (20 mg in a Schlenk tube) at 70 °C under vacuum for 24 h. The resulting orange powder was characterized by multinuclear NMR. **3** is very air-sensitive.

^{1}H NMR (300.13 MHz, C_6D_6, 298 K): δ = 8.74 (d, 1 H, Pyr, $^3J_{HH}$ = 4.8), 6.99 (ddd, 1 H, Pyr, $^3J_{HH}$ = 6.9, $^3J_{HH}$ = 8.4, $^4J_{HH}$ = 1.8), 6.76 (d, 1 H, Pyr, $^3J_{HH}$ = 8.1), 6.28 (ddd, 1 H, Pyr,, $^4J_{HH}$ = 0.9), 5.25 (hept, 1 H, SiH, $^3J_{HH}$ = 3.6, $^1J_{HSi}$ = 204), 2.22−1.20 (m, 66H, PCy_3), 0.83 (s, 6H, Ru−$SiMe_2$); 0.53 (d, 6 H, HSi$\underline{Me}_2$, $^3J_{HH}$ = 3.6). −12.70 (t, RuH, $^2J_{HP}$ = 25, $^2J_{HSi}$ = 11). ^{13}C{^{1}H} NMR (75.47 MHz, C_6D_6, 298 K): δ = 167.08, 150.46, 132.22, 111.41, 110.67 (all for Pyr), 36.66 (t, $^1J_{PC}$ = 6.4, PCH), 31.70, 30.09, 28.32, 26.88 (all for CH_2 of PCy_3), 12.78 (s, $SiMe_2Ru$), −2.32 ($SiMe_2H$). ^{31}P{^{1}H} NMR (121.49 MHz, C_6D_6, 298 K): 52.7 (s, PCy_3); ^{29}Si HMQC NMR (59.6 MHz, C_6D_6, 298 K): δ = −16.6 ($SiMe_2H$); 64.1 (Ru−$SiMe_2$) and ^{29}Si HMQC NMR (79.49 MHz, Tol-d_8, 233 K): δ = −15.9 ($SiMe_2H$); 65.0 (Ru−$SiMe_2$).

Anal. Calcd. for $RuC_{45}H_{84}N_2Si_2P_2$: C, 61.96; H, 9.71; N, 3.21. Found: C, 62.24; H, 10.24; N, 3.07.

Synthesis and Characterization of RuH{$(SiMe_2)N(\kappa N$-$C_5H_4N)$-$(SiMe_2H)$}$_3$ (4). To a solution of Ru(COD)(COT) (120 mg, 380 μmol) in 8 mL of pentane placed in a Fischer−Porter bottle, 3 equiv of **1** were added (240 mg, 1.140 mmol). The solution was pressurized under 3 bar of H_2. After 10 min a solid precipitated. After 14 h the pressure was released, the solution was removed by cannula, and the solid was washed twice with 2 mL of pentane. After drying under vacuum, the pale cream-yellow compound **4** was isolated in 60% yield (166 mg).

^{1}H NMR (500.33 MHz, C_6D_6, 298 K): δ = 7.68 (dd, 1 H, Pyr, $^3J_{HH}$ = 6.0, $^4J_{HH}$ = 2.1), 6.96 (ddd, 1 H, Pyr, $^3J_{HH}$ = 8.7, $^3J_{HH}$ = 6.9, $^4J_{HH}$ = 2.1), 6.81 (d, 1 H, Pyr, $^3J_{HH}$ = 8.4), 6.09 (ddd, 1 H, Pyr, $^3J_{HH}$ = 6.9, $^3J_{HH}$ = 5.7,$^4J_{HH}$ = 1.2), 5.10 (hept, 1 H, SiH, $^3J_{HH}$ = 3.2, $^1J_{HSi}$ = 203.6), 1.10 and 0.30 (2 s, 6H, Ru−$SiMe_2$), 0.48 and 0.40 (2 d, 6H, $NSiHMe_2$, $^3J_{HH}$ = 3.6); −13.63 (s, 1 H, Ru−H, J_{SiHapp} = 7.5). ^{13}C{^{1}H} NMR (125.82 MHz, C_6D_6, 298 K): 166.4, 149.1, 135.9, 112.8, 112.4 (all for Pyr), 11.9($RuSiMe_2$), 5.64 ($RuSiMe_2$), −2.1($NSiMe_2H$), −2.4 ($NSiMe_2H$). ^{29}Si HMBC and HMQC NMR (99.39 MHz, C_6D_6, 298 K): −14.24 ($SiMe_2H$), 64.94 (Ru−$SiMe_2$). IR (Nujol mulls, cm^{-1}): 2185 (s, νSi−H).

Anal. Calcd for $RuC_{27}H_{52}N_6Si_6$: C, 44.40; H, 7.17; N, 11.50. Found: C, 44.42; H, 7.10; N, 10.74.

Neutron Structure Determination of 4. A prismatic, dark-yellow crystal, with an approximate volume of 4 mm^3, was mounted in an inert Ar atmosphere between two wads of quartz wool inside a thin-walled quartz tube, sealed with an O-ring to a purpose-designed Al base.[43] The sample was mounted on a Displex cryorefrigerator on the ILL thermal-beam diffractometer D19 equipped with the new horizontally curved "banana-shaped" position-sensitive detector.[44] This detector is based on a multiwire gas counter technology (5 atm ^{3}He and 1 atm CF_4), with innovative use of an electrostatic lens to improve vertical resolution, and subtends 30° vertically and 120° horizontally. The read-out of 256 pixels (vert.) and 640 pixels (horiz.) gives a nominal spatial definition of 1.56 mm (vert.) and 2.50 mm(horiz.), although the actual resolution is about 3 mm. This detector is mounted symmetrically around the equatorial plane, with a sample-to-detector distance of 76 cm. This new setup assures accurate data and fast data collection times even with "small" size crystals (≤1 mm^3). The crystal was cooled slowly (2 K/min), while monitoring the diffraction pattern, to 20 K. The space group $R\bar{3}$ was confirmed at 20 K. No significant changes in the crystal mosaic or splitting of the peaks were observed during cooling. The chosen neutron wavelength of 1.16954(2) Å from the Cu(331) planes of a Cu (220)-cut monochromator in reflection (at the high resolution 90° takeoff angle) was accurately determined by refining the 2θ values of 2272 reflections from a DKDP standard crystal. The accessible intensities, up to $2\theta \leq 123.38°$, were measured, to preset monitor counts, in a series of 80° ω scans, in steps of 0.07° and typical counting times of 16 s per step; this rather long time-per-frame was considered necessary to obtain reasonable counting statistics. A wide range of crystal orientations (different ϕ and χ positions) was used to cover reciprocal space with massive redundancy as a test of both the sample and the detector stability. Because of its large horizontal opening, only one detector position was required. Between the long scans, 10 strong reflections were monitored every 8 h in shorter scans and showed no significant change. The unit cell dimensions were calculated precisely (ILL program Rafd19) at the end of the data collection, from the centroids in 3D of 2535 strong reflections ($5.5 \leq 2\theta \leq 122.0°$). We note that the total time for the reported 20 K experiment was less than 3 days, compared to a typical 7−9 days data collection time for a similar experimental setup using the previous detectors. It is also interesting to notice that the mean

(43) Archer, J.; Lehmann, M. S. *J. Appl. Crystallogr.* **1986**, *19*, 456.
(44) Buffet, J. C.; et al. *Nucl. Instrum. Methods Phys. Res. A* **2005**, *554*, 392–405.

number of reflections present in any one frame (a function of both the wavelength used and the cell volume) was about 40. Raw intensity data were corrected for vertical and horizontal positional distortions, and Bragg intensities were integrated in 3D using a new version of the program Retreat,[45] modified for the new detector geometry. For the 2510 strongest reflections the mean positional errors for the centroids were 0.03°, 0.03° and 0.04° (in the scan, horizontal and vertical directions, respectively). In all 13183 Bragg reflections were obtained, of which 4258 were independent. The Bragg intensities were corrected for attenuation by the cylindrical aluminum and vanadium Displex heat-shields (minimum and maximum transmission coefficients 0.9066 and 0.9625). Further crystallographic data and experimental details are given in Table 1 and in the CIF file. The starting structural model for the refinement was based on the atomic coordinates for the heavy atoms taken from the X-ray structural determination. The structure was refined by full matrix least-squares, minimizing the function $[\sum w(F_o^2 - (1/k)F_c^2)^2]$ and using all the independent data. The final structure model included coordinates and anisotropic displacement parameters for all atoms. No extinction correction was deemed necessary. Upon convergence the final Fourier difference map showed no significant features. The coherent scattering amplitudes used were those tabulated by Rauch and Waschkowski.[46] Calculations were carried out by using the PC version of the programs SHELX-97,[47] WINGX and ORTEP[48,49]

Computational Details. DFT calculations were performed with the GAUSSIAN 03 series of programs[50] using the nonlocal hybrid functional denoted as B3PW91.[51,52] For compounds **2a**, **2b** and **2c**, the core electrons of ruthenium were represented by a relativistic small core pseudopotential using the Durand/Barthelat method.[53] The 16 electrons corresponding to the 4s, 4p, 4d and 5s atomic orbitals were described by a (7s,6p,6d) primitive set of Gaussian functions contracted to (5s,5p,3d). Standard pseudopotentials developed in Toulouse were used to describe the atomic cores of all other non-hydrogen atoms (C, N, Si and P).[54] A double plus polarization valence basis set was employed for C, N, Si and P (d-type function exponents were 0.80 for C atom and 0.45 for N, Si and P atoms). For hydrogen, a standard primitive (4s) basis contracted to (2s) was used. A p-type polarization function (exponent 0.9) was added for the hydrogen atoms directly bound to ruthenium and silicon. The geometry of the various critical points on the potential energy surface was fully optimized with the gradient method available in GAUSSIAN 03. Calculations of harmonic vibrational frequencies were performed to determine the nature of each critical point. The calculations on **4** have also been performed at the B3PW91 level. The ruthenium and silicon atoms were represented by the relativistic effective core potential (RECP) from the Stuttgart group and their associated basis set,[55,56] augmented by polarization functions ($\alpha_f = 1.235$, Ru; $\alpha_d = 0.284$, Si).[57,58] The remaining atoms (C, H, N) were represented by 6-31G(d,p) basis sets.[59] Full optimizations of geometry without any constraint were performed. Calculations of harmonic vibrational frequencies were performed to determine the nature of each extrema. Due to the absence of symmetry, the data reported in Table 3 correspond to an average of the different bond distances and angles.

Acknowledgment. We thank the CNRS and the ANR (programme blanc ANR-06-BLAN-0060-01) for support (M.G., L.V., S.S.E.). This work is also supported by the European network IDECAT. A generous allocation of computer time was given by the CINES (Montpellier, France) and CALMIP (Toulouse, France), and A.A. acknowledges support from the MIUR, PRIN 2007 program.

Supporting Information Available: X-ray and neutron crystallographic files for **2** and **4** (CIF). Computational details and Cartesian coordinates for the calculated structures. Complete refs 44 and 50.This material is available free of charge via the Internet at http://pubs.acs.org.

JA901140V

(45) Wilkinson, C.; Khamis, H. W.; Stansfield, R. F. D.; McIntyre, G. J. *J. Appl. Crystallogr.* **1988**, *21*, 471–478.
(46) Rauch, H.; Waschkowski, W. Neutron Scattering Lengths In *Neutron Data Booklet*; Dianoux, A.-J.; Lander, G., Eds.; Institut Laue-Langevin: Grenoble, July 2003; available on line at http://www.ill.eu.
(47) Sheldrick, G. M. *Acta Crystallogr.* **2008**, *A64*, 112–122.
(48) Farrugia, L. J. *J. Appl. Crystallogr.* **1999**, *32*, 837–838.
(49) Farrugia, L. J. *J. Appl. Crystallogr.* **1997**, *30*, 565.
(50) Frisch, M. J.; et al. Gaussian 03, Revision C02; Gaussian, Inc.: Wallingford, CT, 2004.
(51) Becke, A. D. *J. Chem. Phys.* **1993**, *98*, 5648–5652.
(52) Perdew, J. P.; Wang, Y. *Phys. Rev. B* **1992**, *45*, 13244–13249.
(53) Durand, P.; Barthelat, J. C. *Theor. Chim. Acta* **1975**, *38*, 283–302.
(54) Bouteiller, Y.; Mijoule, C.; Nizam, M.; Barthelat, J. C.; Daudey, J. P.; Pelissier, M.; Silvi, B. *Mol. Phys.* **1988**, *65*, 295–312.
(55) Andrae, D.; Häussermann, U.; Dolg, M.; Stoll, H.; Preuss, H. *Theor. Chim. Acta* **1990**, *77*, 123–141.
(56) Bergner, A.; Dolg, M.; Kuchle, W.; Stoll, H.; Preuss, H. *Mol. Phys.* **1993**, *80*, 1431–1441.
(57) Ehlers, A. W.; Böhme, M.; Dapprich, S.; Gobbi, A.; Höllwarth, A.; Jonas, V.; Köhler, K. F.; Stegmann, R.; Veldkamp, A.; Frenking, G. *Chem. Phys. Lett.* **1993**, *208*, 111–114.
(58) Höllwarth, A.; Böhme, H.; Dapprich, S.; Ehlers, A. W.; Gobbi, A.; Jonas, V.; Köhler, K. F.; Stegmann, R.; Veldkamp, A.; Frenking, G. *Chem. Phys. Lett.* **1993**, *208*, 237–240.
(59) Hariharan, P. C.; Pople, J. A. *Theor. Chim. Acta* **1973**, *28*, 213–222.